BULLETIN OF THE EARTHQUAKE
RESEARCH INSTITUTE
Vol. 37 (1959), pp. 39-51

4. *Physical Conditions of Earthquake Faults II.*

(*A Model of Strike-slip Faults with Various Dip Angles.*)

By Keichi KASAHARA,

Earthquake Research Institute.

(Read December 23, 1958.—Received December 27, 1958.)

Summary

The writer deals with a model of strike-slip faults for the purpose of studying the characteristics of crustal deformation when the dip of the fracture plane is not given as 90°. The model is presented on the assumptions which are similar to those in the previous paper, but no assumption on the dip angle is made in the present one. An orthodox analysis of such a model being very difficult even in the simplest case, the writer reduces the problem to the Laplace equation and solves it by the relaxation method as well as by model experiments based on the electric-elastic analogy.

It is proved that the pattern of deformation is no more symmetric with respect to the fault but the deformation on the side of the fault, to which it dips, appears systematically larger than that of the other side. The more the dip angle differs from 90°, the more remarkable the asymmetry becomes.

We are able to point out some examples, the deformation in which is likely to be explained more suitably by the present model rather than by the primary one. However, definite conclusions on that point will be postponed until we accomplish more detailed examination.

1. Introduction

It is widely accepted that the crustal deformation around an earthquake fault is closely related to the characteristics of the earthquake origin. Notwithstanding a great store of geodetic data, however, few papers have been written until L. Knopoff[1], P. Byerly and J. DeNoyer[2],

1) L. KNOPOFF, *Geophys. Journ., R.A.S.*, **1** (1958), 44-52.

2) P. BYERLY and J. DENOYER, *Contributions in Geophysics in Honor of B. Gutenberg* (1958), 17-35.

and the present writer[3] worked out studies, in which physical conditions of several faults were discussed on the basis of these observational data. Since it was hardly possible to deal with such complicated features of actual faulting in detail, the above-mentioned writers took very simplified models representing only the most predominant conditions of strike-slip faults.

The present writer's model assumed, for instance, the fracture plane in the earth's crust to be of infinite length and of finite (constant) depth, in which the initial shear stress is liberated. For the sake of simplicity in mathematical analysis, it was also assumed that the fault appears with a dip of 90°. The foregoing analyses have proved that the above-mentioned model can provide satisfactory explanation for the most outstanding features of some actual faultings, so that it may be accepted as a reasonable model in the step of first approximation.

It is needless to say that such a conclusion has been stated by disregarding some sorts of discrepancy from the observational facts, which should be taken into account when we undertake further improvement of the model. One of the discrepancies is noticed in the diminution curve of v_0. The primary model concludes that the curves for both sides of a fault are to be perfectly antisymmetric with each other, in the absence of the distortion due to the elastic drift in the earth's crust. The distribution of v_0 on the east and west sides of the Imperial Valley fault (or of the Fairview Peak fault) is likely to be represented more suitably by the two curves of different diminution rather than by curves of the same diminution (see Figs. 4 and 6 in the previous paper). Such a tendency can not be explained so long as we take the primary model which assumes the dip to be 90°. One of the way to overcome this difficulty might be to do away with the assumption on the dip angle, so that we are going to deal with the model improved in the following way.

2. Fundamental considerations

The model cited here is on the same assumptions as the primary one except that on the dip angle (φ) of the fracture plane (Fig. 1). Let us take the symbols for coordinates, displacements, and elastic constants as same with those in the former papers, then the condition of elastic equilibrium is given by the following equations,

3) K. KASAHARA, *Bull. Earthq. Res. Inst.*, **35** (1957), 473-532; *ibid.*, **36** (1958), 21-53; *ibid.*, **36** (1958), 455-464.

$$\left.\begin{aligned}(\lambda+\mu)\frac{\partial}{\partial x}\Delta+\mu\left(\frac{\partial^2}{\partial x^2}+\frac{\partial^2}{\partial y^2}+\frac{\partial^2}{\partial z^2}\right)u=0\ ,\\(\lambda+\mu)\frac{\partial}{\partial y}\Delta+\mu\left(\frac{\partial^2}{\partial x^2}+\frac{\partial^2}{\partial y^2}+\frac{\partial^2}{\partial z^2}\right)v=0\ ,\\(\lambda+\mu)\frac{\partial}{\partial z}\Delta+\mu\left(\frac{\partial^2}{\partial x^2}+\frac{\partial^2}{\partial y^2}+\frac{\partial^2}{\partial z^2}\right)w=0\ .\end{aligned}\right\} \quad (1)$$

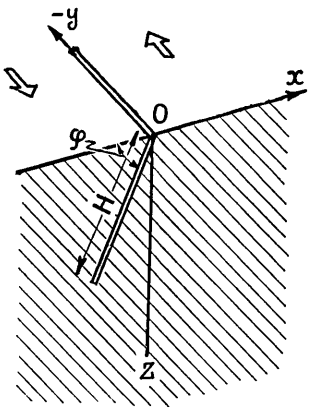

Fig. 1. Model of a strike-slip fault.

It is evident, from the physical considerations, that the deformation is uniform in the direction of y, that is,

$$\frac{\partial}{\partial y}\equiv 0\ . \quad (2)$$

Eq. (1) can be rewritten, then, as follows,

$$\mu\left(\frac{\partial^2}{\partial x^2}+\frac{\partial^2}{\partial z^2}\right)v=0\ , \quad (3)$$

and,

$$\left.\begin{aligned}(\lambda+2\mu)\frac{\partial^2 u}{\partial x^2}+(\lambda+\mu)\frac{\partial^2 w}{\partial x\partial z}+\mu\frac{\partial^2 u}{\partial z^2}=0\ ,\\(\lambda+2\mu)\frac{\partial^2 w}{\partial z^2}+(\lambda+\mu)\frac{\partial^2 u}{\partial x\partial z}+\mu\frac{\partial^2 w}{\partial x^2}=0\ .\end{aligned}\right\} \quad (4)$$

We know, therefore, that the fundamental equations are given for u and w separately from that for v. Since the model assumes no initial stress except a uniform shear, Y_x, it is only the stress component relating to v that is liberated in the fracture plane, whereas no change occurs in the other components relating to u and w, there. Taking these conditions into account, we may take as,

$$u=w=0\ , \quad (5)$$

which does not contradict (4) as well as the initial and the boundary conditions stated above. That is to say, the deformation in the present model is represented by a pure shear field.

Let us introduce the potential of the field, ϕ, which satisfies the Laplace equation,

$$\nabla^2\phi=0\ , \tag{6}$$

and is related to v as follows.

$$\frac{\partial v}{\partial x}=-\frac{\partial \phi}{\partial z}\ , \qquad \frac{\partial v}{\partial z}=\frac{\partial \phi}{\partial x}\ . \tag{7}$$

This is also the relation between the stream function ψ and the potential. The boundary condition for v or ϕ at the free surface is given, then,

$$\frac{\partial v}{\partial n}=0 \qquad \text{or} \quad \phi=\text{const.}, \tag{8}$$

where, n is the direction normal to the surface.

3. Solution by relaxation method

The fundamental considerations have shown that the problem with which we are concerned is reducible to that of a potential field. The solution for the problem should satisfy the Laplace equation within the medium, and, at the same time, the conditions for a free surface in the fracture as well as at the earth's surface. With the aid of (8), it is evident that ϕ is constant (we suppose it as 0) in these planes. From the physical point of view, we also know that the value of ϕ approaches Cz (C is a constant) at a great distance from the fault.

The relaxation method is useful for solving such a problem. In case of $\varphi=60°$, for instance, it is convenient to deal with the numerical calculation with respect to the triangular network (Fig. 2). The operator ∇^2 is expressed in polar coordinates as follows.

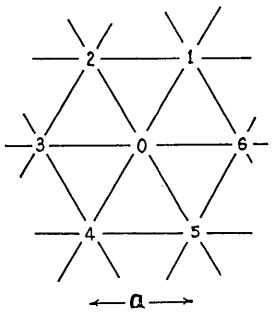

Fig. 2. Relaxation net ($N=6$).

$$\nabla^2\equiv\frac{\partial^2}{\partial r^2}+\frac{1}{r}\frac{\partial}{\partial r}+\frac{1}{r^2}\frac{\partial^2}{\partial\theta^2}\ . \tag{9}$$

Let us also take the expression for ϕ in the expanded forms, that is,

$$\phi(r,\ \theta)=A_0(r)+\sum_n \{A_n(r)\cos n\theta+B_n(r)\sin n\theta\}\ . \tag{10}$$

Hence we get,

$$\nabla^2\phi=A_0''+\frac{1}{r}A_0'+\sum_n\left\{\left(A_n''+\frac{1}{r}A_n'-\frac{n^2}{r^2}A_n\right)\cos n\theta\right.$$
$$\left.+\left(B_n''+\frac{1}{r}B_n'-\frac{n^2}{r^2}B_n\right)\sin n\theta\right\}, \qquad (11)$$

where, the symbols $'$ and $''$ denote $\partial/\partial r$ and $\partial^2/\partial r^2$, respectively.

Let $\sum_{a,N}(\phi)$ denote the summation of ϕ at the nearest net points which are at equal distances from the point 0, $r=a$ (a is the length of the mesh-side and $a\ll 1$), then, we get[4],

$$\frac{1}{N}\sum_{a,N}(\phi)=A_0(a)+O(a^N)+\cdots, \qquad (12)$$

and

$$A_0(r)=\phi_0+\frac{r^2}{4}(\nabla^2\phi)_0+\frac{r^4}{64}(\nabla^4\phi)_0+\cdots, \qquad (13)$$

where, the suffix 0 corresponds to the point 0 and N is the number of the nearest network points ($N=6$ in the present case). Therefore, by neglecting the terms of higher powers of a we arrive at the following relation,

$$\frac{1}{N}\sum_{a,N}(\phi)-\phi_0\fallingdotseq\frac{a^2}{16}\left[\left(3\nabla^2\phi+\frac{1}{N}\sum_{a,N}(\nabla^2\phi)\right)\right]. \qquad (14)$$

That is to say, when the Laplace equation is satisfied by ϕ, (6) is reduced to the following relation of finite-difference form, *viz.*,

$$\frac{1}{N}\sum_{a,N}(\phi)-\phi_0=0\ . \qquad (15)$$

In the relaxation method, we first assume the first approximation values of ϕ for all the net points, and calculate the residual of the left-hand side of (15) for each point. The residual is fed back, then, to the assumed values at all the surrounding points in order to take the second approximation values. Such a procedure is repeated until we look for the most suitable values which satisfy (15) at all points.

In the present study we take the depth of the fault, H, as the unit distance and the length of the mesh-side, a, as 1/8 of the unit. Fig. 3 illustrates the relaxation net and the equal-value lines of ϕ in relative values thus calculated. Since it is not ϕ but ψ that corresponds

4) R. V. SOUTHWELL, *Relaxation Methods in Theoretical Physics I* (1946), p. 20.

to v, we have to deduce the distribution of ψ from the result shown in Fig. 3. This procedure is easily accomplished with the aid of the relation between ϕ and ψ (cf. (7)), so that we finally obtain the pattern for ψ as shown in Fig. 4.

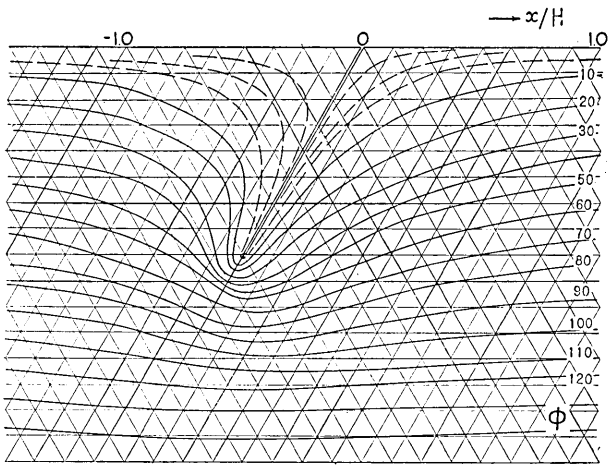

Fig. 3. Relaxation net and distribution of ϕ.

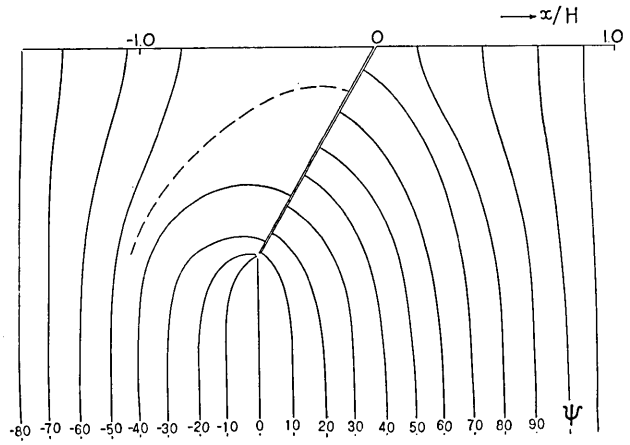

Fig. 4. Distribution of ϕ.

The distribution which is directly related to the faulting is known as the difference of the pattern in Fig. 4 from the one before faulting. We know, therefore, that it is only the part nearby the fault that is subject to remarkable deformation, whereas the part away from there

is unaffected as the distribution of parallel lines indicates. The lines approaching the earth's surface or the fracture plane are normal to the respective boundaries, which means that the condition for the free surface (8) is satisfied. The most notable effect is the asymmetric distribution around the fault. It is evident that the deformation in the left half part of the space is larger than that in the other half. This tendency being in good agreement with the result of the following model experiment, we shall discuss it in more detail in the next section.

4. Model experiment based on electric-elastic analogy

The relaxation method is applicable, in principle, not only to the case of $\varphi=60°$ but also to the other cases. Numerical computation would be, however, more complicated in such case, so that we shall take another way in order to study the present problem easily.

L. Knopoff has shown that the analogy of an electrostatic field is applicable to the problem of a pure shear field (see Table 1)[5]. Taking

Table 1. Two-dimensional analogies (after L. Knopoff).

Electric quantity	Elastic quantity
Electric field	Rotation vector
Dielectric constant	Shear modulus
Potential	Potential
Stream function	Displacement
Perfect conductor	Perfectly weak crack

this analogy into consideration, we are able to find out, experimentally, the solution for various values of φ by inserting a conductor of proper shape into a uniform electric field and by tracing equi-value lines of ϕ around it. The technique using a thin layer of electrolyte has frequently been applied to studies of electrostatic field around a conductor. It is a necessary condition for the technique that the resistivity of the electrolyte is far higher than that of the electrode which forms the conductor under the test. Let us call such a type a conductor model of the electrostatic field.

The technique applied in the following study is the one using an insulator model, in which the objective is not given by a conductive electrode but is represented by an insulator of the same shape. As is

5) L. KNOPOFF, *loc cit.*, 1).

well-known, the equipotentials of an electrostatic field (or of a field of stationary current) are normal to the stream lines, and the former is normal to the boundary of an insulator as the latter is, to a conductor. Therefore, the pattern of the stream lines in a conductor model must be identical with that of the equi-potential lines in an insulator model, when the above-mentioned correspondence holds between them.

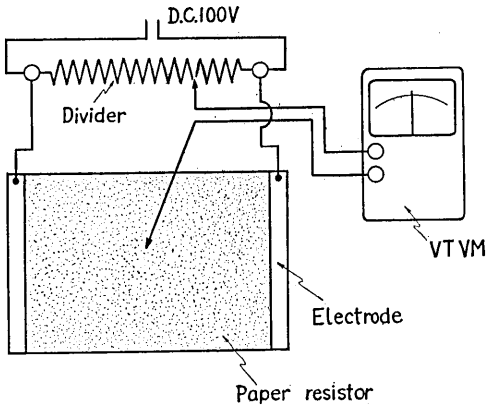

Fig. 5. Laboratory set of model experiment.

Fig. 5 illustrates the laboratory set using an insulator model. A sheet of paper resistor (26 cm × 37 cm) is in contact with the electrodes at its ends, to which D.C. voltage (100 V) is supplied. Then the potential is of a constant gradient from one electrode to the other, and the equi-potential lines appear normally to the upper rim of the paper resistor, which corresponds to the surface of the earth. This represents the initial state of the earth's crust being subject to uniform shear stress, $Y_x = S$.

Production of a fracture is represented by applying a narrow cut from the upper rim of the resistor to a certain depth. This cutting causes distortion of the equi-potential lines, which are traced with a VTVM connected to a potential divider as shown in the same figure. Since the input resistance of this apparatus is extremely high, we can trace distribution of the potential ϕ without disturbing the condition of the field. Uniformity of resistivity in the test paper has much influence upon the accuracy of the experimental result. Facsimile paper is used in the present experiment, as it shows uniform and suitable resistivity. This method of experiment being very simple in its treatment, it could be conveniently applied to the other sorts of problems which relates to the Laplace equation.

5. Result and discussions

We worked out the model experiment for the cases of $\varphi = 90°$, 80°, 70° and 60°, where the depth of cutting was kept unchanged ($H = 10$ cm). The results are shown in Figs. 6~9. The lower part of each figure il-

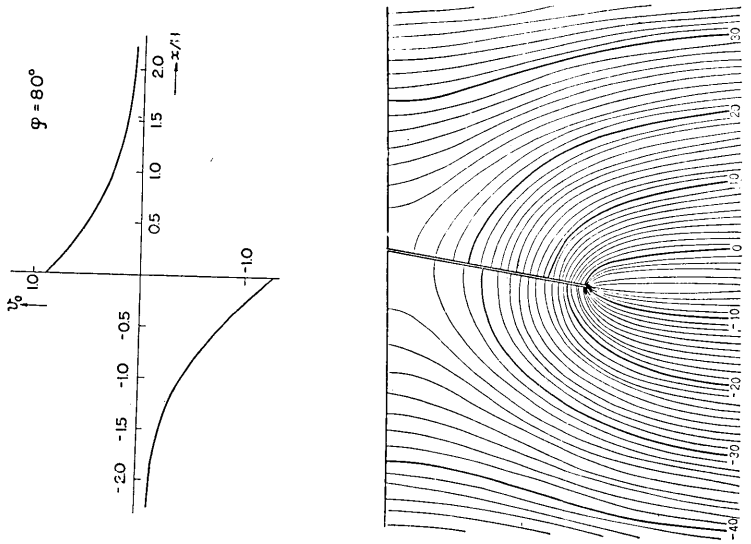

Fig. 7. Distribution of v and v_0 ($\varphi=80°$).

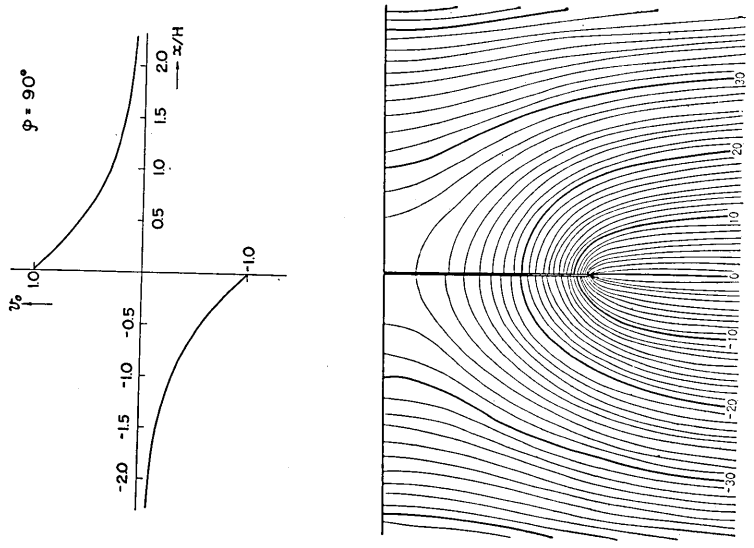

Fig. 6. Distribution of v and v_0 ($\varphi=90°$).

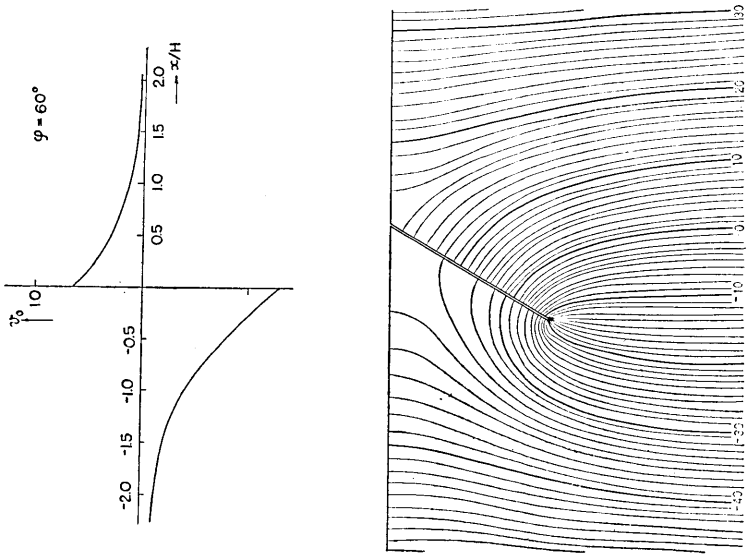

Fig. 9. Distribution of v and v_0 ($\varphi=60°$).

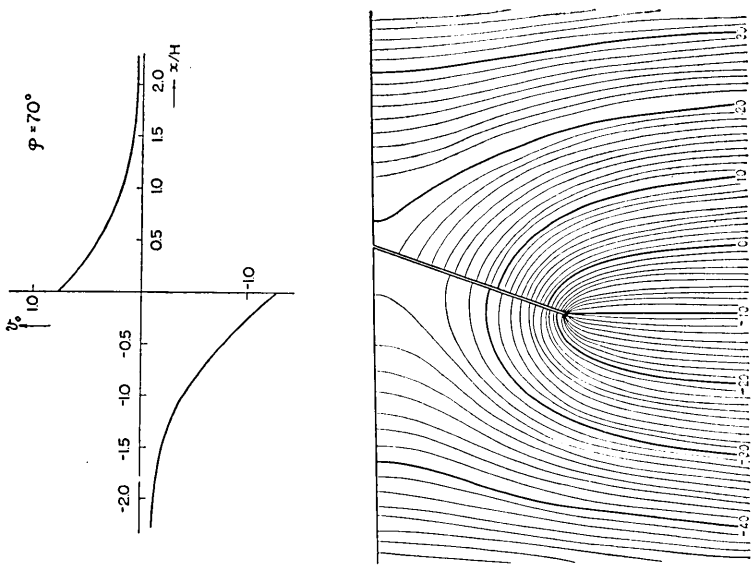

Fig. 8. Distribution of v and v_0 ($\varphi=70°$).

lustrates the distribution of electric potential in the insulator model, so that it should be understood as the distribution of v in the elastic model. The pattern itself indicates the deformation due to the faulting overlapped by the initial deformation, so that we have to subtract the latter effect in order to see the former effect only. The curve in the upper part of the figure is for one which illustrates the diminution of v_0 with dimensionless distance x/H.

First we see Fig. 6, in which is shown the distribution pattern when $\varphi=90°$. This is the case that has been discussed in the previous papers. The pattern is symmetric with respect to the fault. It also indicates that the maximum deformation appears in the uppermost part of the fault whereas the maximum stress is at the bottom. It also shows that no remarkable deformation appears at points apart from the fault, say $x/H=1$ or more. The diminution curve drawn in the upper part of the figure is of the same tendency with that obtained from the former analysis.

The distribution pattern is no more symmetric in the case of $\varphi=80°$ (Fig. 7). The deformation in the left half space, to which the fault dips, is more remarkable than that in the opposite side one. This tendency of asymmetry can be seen more concretely in the diminution curve,

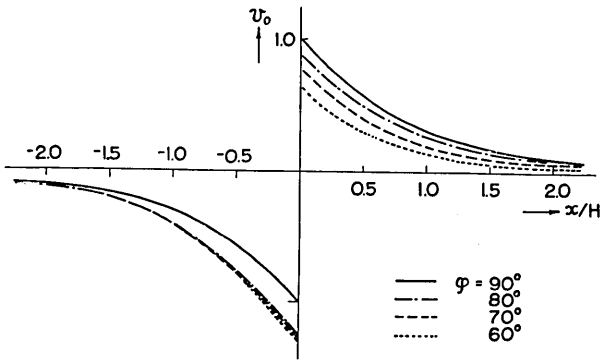

Fig. 10. Diminution curves for various values of φ.

the ordinate of which is scaled taking the value of v_0 at $x=0$ when $\varphi=90°$ as the unit. The more the dip deviates from 90°, the more remarkable the asymmetry becomes. Such a tendency can be seen clearly by drawing the curves for various values of φ in the same coordinates (Fig. 10).

We have mentioned, in the first section of this paper, a notable

characteristic of diminution curves in the cases of the Imperial Valley fault and the Fairview Peak fault. In each of these cases triangulation stations on the east side of the fault shifted more than those on the opposite side (see Figs. 4 and 6 in the previous paper). It is needless to say that this tendency can not be attributed to the elastic drift in the earth's crust, because the interval between the surveys before and after the faulting was very short in the said cases and v_0 approaches 0 with the increase of x. The asymmetric distribution of v_0 concluded from the present model is likely to provide a more reasonable explanation for the mentioned effect. Especially in the case of the Fairview Peak fault, a notable data has been reported by C. Romney, who investigated the fault-plane solution for the earthquake[6]. According to his result, the fault plane is likely to dip as much as 65° to east. This sense of dipping to east agrees well with the above-mentioned tendency of the diminution curve, although the larger angle (80° or so) is likely to be concluded from the present model. We would not like to develop further discussion here, as we have no more concrete data for comparison. Definite conclusions will be postponed until we accomplish detailed examination in future.

6. Acknowledgement

The writer wishes to acknowledge the valuable advice and suggestions for the present study kindly given by Dr. T. Rikitake of this Institute. The writer's thanks are also extended to Mr. I. Tanaoka and Miss R. Iwaya for their kind assistance in the course of the study.

---

4. 地震断層の性状について (2)

(dip が 90° でない場合の断層模型)

地震研究所 笠 原 慶 一

横ずり型であり，且つその dip が 90° であるような断層模型については，既に前報においてその基本的特性を考察し，いくつかの実例に対する比較をも試みて来た．今回はこの模型を拡張して dip が 90° でない場合にどういう特性の地殻変動（水平移動）が期待されるかを調べたものである．

このような力学模型に対する解析的な解を求めることは極めて困難であるから，dip が 60° の場合については relaxation method による数値解法を行い，更に一般の場合については (φ=90°～60°) 電場とずり歪の場との類似性に基づく模型実験を行つた．

6) C. ROMNEY, *Bull. Seis. Soc. Amer.*, **47** (1957), 301-320.

$\varphi=90°$ の場合に対する実験結果は，当然のことながら，既報の計算結果とよく一致する．dip が 90° でなく，断層面がどちらかの側に傾いていると，その側の変動は他方の側のそれよりも顕著に現われる．従つてこの場合，$\varphi=90°$ の模型について見られたような変動の対称性（逆対称性）はもはや認められない．断層面の深さを一定に保ちながら，φ の変化による変動分布の特性を比較して見ると，φ が 90° を遠ざかる程非対称性が目立つて来る．

今回の模型では辷り歪力の役割のみを強調して，他の歪力成分（例えば地殻中に存在する静水圧的な歪力等）の影響を無視する立場をとつている．従つて今回の結果をそのまま現実の地殻に適用することには問題が残されているが，φ が 90° から余り離れていない範囲で dip 変化の影響を考察する限り充分参考になるであろう．

実際の地殻変動の分布（三角点の水平移動）を詳細に検討して見ると，その分布曲線が断層の両側で完全な逆対称でない場合が認められる（前報所載の Imperial Valley 断層や Fairview Peak 断層の場合等）．これらの地震断層の dip について明確な資料が得られない現状で断定的な議論をすることは差し控えたいが，例えば後者の場合，地震波の押し引き分布から推定される断層面は東側に傾いていたという報告もある．それが事実とすれば定性的には上記模型と適合することになる．より詳細な検討については今後の研究を進めたい．

尚，今回採用した電場模型の実験方法は，電解液と交流ブリッジとを組み合わせて行う従来のものと原理的に若干異なつており，実用上便利な点が多い．Laplace 方程式に関する各種の問題に広く適用することができると思う．